Optimal ferromagnetically-coated carbon nanotube tips for ultra-high resolution magnetic force microscopy

Y. Lisunova[1], J. Heidler[2], I. Levkivskyi[3,4], I. Gaponenko[1], A. Weber[2], L.J. Heyderman[2], M. Kläui[2,5], C.Caillier[1] and P. Paruch[1]

[1] DPMC-MaNEP, University of Geneva, 24 Quai Ernest-Ansermet, 1211 Geneva 4, Switzerland

[2] Paul Scherrer Institut , 5232 Villigen PSI, Switzerland

[3] DPT, University of Geneva, 24 Quai Ernest-Ansermet, 1211 Geneva 4, Switzerland

[4] Bogolyubov Institute for Theoretical Physics, 03680 Kiev, Ukraine

[5] University of Mainz, Institute of Physics, Staudinger Weg 7, 55128 Mainz, Germany

E-mail: `Yuliya.Lisunova@unige.ch`

Abstract. Using single-walled carbon nanotubes homogeneously coated with ferromagnetic metal as ultra-high-resolution magnetic force microscopy probes, we investigate the key image formation parameters and their dependence on coating thickness. The crucial step of introducing molecular beam epitaxy for the magnetic coating deposition allows highly controlled fabrication of tips with small magnetic volume, while retaining high magnetic anisotropy and prolonged lifetime characteristics. Calculating the interaction between the tips and a magnetic sample, including hitherto neglected thermal noise effects, we show that optimal imaging is achieved for a finite, intermediate-thickness magnetic coating, in excellent agreement with experimental observations. With such optimal tips, we demonstrate outstanding resolution, revealing sub-10 nm domains in hard magnetic samples, and non-perturbative imaging of spin structures in soft magnetic materials, all at ambient conditions with no special vacuum, temperature or humidity controls.

PACS numbers: 68.37, 75.75, 81.07, 75.70

1. Introduction

Intense fundamental and applied research on nanomagnetic materials and devices has generated an increasing demand for ultra-high resolution, non-invasive imaging of magnetic domain nanostructures [1, 2, 3, 4]. In particular, to keep pace with continuously improving magnetic recording media, currently in the Tbit/in^2 range [5], the ability to resolve sub-10 nm magnetic features is a necessity. In parallel, for imaging of complex spin structures in soft magnetic samples [6, 7, 2, 8, 9, 10], especially in device geometries such as racetrack memories [3], a weak probe-sample interaction is required to minimize disturbance of the magnetic configuration. Magnetic force microscopy (MFM) is commonly used due to its high resolution and convenience, with significant enhancement in imaging efficiency due to the recent introduction of ferromagnetic-thin-film-coated carbon nanotube (MFM-CNT) tips [11, 12, 13]. The combination of the small diameter and high aspect ratio of carbon nanotubes results in the formation of a well defined magnetic volume with high anisotropy, allowing both soft and hard magnetic materials to be accessed [11, 12, 14, 15, 13, 16]. The small volume of magnetic metal coating at the tip leads to improved resolution, with magnetic domains in storage media imaged at ultra-high densities from 700 to 1400 kFCI (350 Tbit/in^2)[13, 16]. Meanwhile, the magnetic field of such tips is sufficiently weak not to perturb the magnetization of permalloy thin film microstructures, allowing the nanoscale observation of vortex cores and domain walls in these materials [15].

For the highest quality images, understanding and optimizing not only the MFM-CNT tips themselves, but also their interaction with the sample is critical. Finite-element simulations of such tips with different CNT diameter and magnetic coating thickness suggest that the highest resolution and most uniform magnetization should be achieved with very thin magnetic coatings of small diameter CNT [16]. However, experimentally, image quality was observed to decrease for smaller probes with thinner coatings [13, 16], suggesting that these simple considerations do not lead to the right choice for optimum results. Significantly better imaging was obtained with an intermediate thickness of the magnetic coating layer. This effect was variously attributed to the influence of decreasing contrast with a smaller magnetic volume, weak magnetic dipole interaction [13] or to discontinuities in the magnetic coating layer resulting in a transition to the superparamagnetic state [16]. To date, however, all the proposed theoretical models are constructed for an ideal situation, neglecting thermal noise and magnetic disorder intrinsically present in real system. Meanwhile, the MFM-CNT experiments were done using multi-walled CNT, whose relatively wide diameters inherently limit the minimum tip size, making a comparison to a point-probe approximation difficult[13], and necessitating more complex models to accurately describe the interaction[16]. Combining a theoretical analysis of MFM-CNT imaging and its limitations in a real system with the development of single-walled CNT-based tips with a highly uniform magnetic coating, and the characterization of the resulting imaging properties is therefore a crucial step to advance this technique, and establish it

as a next-generation tool for magnetic characterization.

In this Letter, we report on such a combined investigation, analyzing both experimentally and theoretically the optimal conditions for MFM imaging in real systems, taking into consideration the inherent physical limitations on sensitivity and resolution. To obtain the highest quality tips, we introduce the deposition of the magnetic metal coating via molecular beam epitaxy on single-walled CNT, allowing unprecedented sub-10 nm resolution under ambient MFM imaging conditions. Theoretically, we model the interaction of such MFM-CNT tips with a magnetic sample in the presence of thermal noise, reconstructing the resulting image, and quantifying the resolution as a function of the magnetic coating thickness, in excellent agreement with experimental observations. The advantages of these magnetic single-walled CNT–based tips are demonstrated on geometrically-confined spin structures in micropatterned soft magnets, as well as on domains in hard magnetic samples.

2. Experimental details

To fabricate the tips, single-walled CNT were grown on commercial Si-based atomic force microscopy probes (*μMasch NSC18*, $\sim$3.5 N/m, $\sim$75 kHz) by chemical vapor deposition [17, 18], resulting in individual CNT or thin bundles 2–5 nm in diameter, 1–5 μm long, at the tip apex. To obtain good image quality, these CNT were shortened by electrical etching at 5–10 V on a sputtered Nb surface, to typical lengths of 300–500 nm. A thin Co film (nominal thickness t_n 5, 10, or 15 nm) was then deposited on the shortened CNT tips by molecular beam epitaxy in ultra high vacuum (10^{-10} mbar) at room temperature, at a rate of 4 nm/hour and 360 degree sample rotation. This very low-rate Co growth on the CNT tips in a clean ultra high vacuum environment resulted in a uniform and homogeneous formation of a well-adhered magnetic metal layer, eliminating any need for preliminary functionalization of the CNT ‡. To prevent the oxidation and deterioration of the thin Co layer, 10 nm Au was subsequently added as a protective coating [11, 19] in-situ, without breaking the vacuum. Scanning electron microscopy (*JEOL 7500*, 2kV) was used to characterize the tip after the Co/Au deposition, as shown in figure 1, confirming the uniform deposition of the metal layer with no discontinuities, and allowing us to directly measure the final tip diameter d_t. Finally, to improve the signal-to-noise ratio of the probe, 8 nm of reflective Al on a 1 nm Ti adhesion layer were electron-beam deposited on the back of the cantilever at a rate of 0.02 nm/s, shielding the tip itself during this step [18]. In this study, a total of 24 different tips were investigated: 8 with average $t_n = 5$ nm, $d_t = 20$ nm; 4 with average $t_n = 10$ nm, $d_t = 25$ nm; and 12 with average $t_n = 15$ nm, $d_t = 30$ nm. The tips survived extended use for over a year, demonstrating the strong adhesion between the CNT and Co and efficiency of the protective Au layer.

To characterize their performance, the MFM-CNT tips were directly compared

‡ As well, MBE is less destructive as compared to the conventional sputtering technique, where single-walled nanotubes can be substantially damaged, buckled and strongly bent in the process of deposition

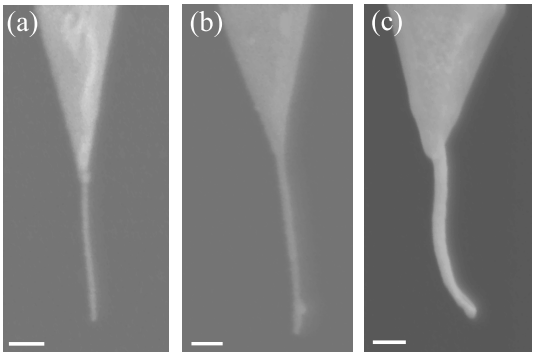

Figure 1. SEM images of MFM-CNT tips homogeneously coated with (a) 5 nm, (b) 10 nm and (c) 15 nm of Co. Scale bar is 100 nm.

with commercial MFM probes (*Veeco MESP*,Cr/Co, ∼2 N/m, ∼70 kHz). The MFM measurements were carried out in a commercial atomic force microscope (*VEECO Dimension 3100* with *Nanoscope V* controller) in standard dynamic (tapping)-lift mode detecting the oscillation phase shift in air at room temperature, where the quality factor of the MFM-CNT tips was approximately 350. The lift height and scan rate were optimized for each probe to obtain the best image. First, to verify the imaging quality of the MFM-CNT tips, and to investigate the effects of varying Co coating thickness, we used a standard hard disk with (perpendicular recording, *Seagate Momentus 5400.6*, nominal bit length 17 nm [18]) with a root-mean-square (rms) surface roughness of 0.2 nm from topography measurements. Using the MFM-CNT tips with the highest resolution, we then extended our studies to square (5×5 μm^2, 25 nm thick) and rectangular (4.5×9 μm^2, 25 nm thick) soft magnetic films with a rms surface roughness of 0.355 nm, in which a variety of more complex spin structures could be accessed [6, 8, 20]. These samples were fabricated by electron beam lithography in combination with a lift-off process from 25 nm-thick films of permalloy (Source Material Ni:Fe, 83:17 wt) deposited by thermal evaporation at a base pressure of 5x10 $^{-6}$ mbar and with a 2 nm Al capping layer on a patterned PMMA (polymethyl methacrylate) resist.

3. Results and discussion

We find that the resolution and contrast of the MFM-CNT images varies significantly with the thickness of the Co layer, in agreement with previous studies of ferromagnetically-coated multiwalled-CNT tips [13, 16]. As shown in figure 2(b), with only 5 nm of Co, it turns out to be difficult to identify individual bits. The small magnetic volume of the tip results in weak tip-sample interaction, giving a signal amplitude comparable to the measurement noise. However, as can be seen in figure 2(c, d), with increasing Co thickness, we observe significant improvement in the signal-to-noise ratio. Bits with a full-width-half-maximum of 18 and 15 nm can be clearly resolved with t_n = 10 and 15 nm Co-coated tips, respectively. Moreover, with t_n = 15 nm Co-coated MFM-CNT tips the characteristic curvature of the individual bits can be detailed with high

precision at sub-10 nm (figure 2(e)). In comparison, the commercial MFM tips show a best resolution of 30 nm.

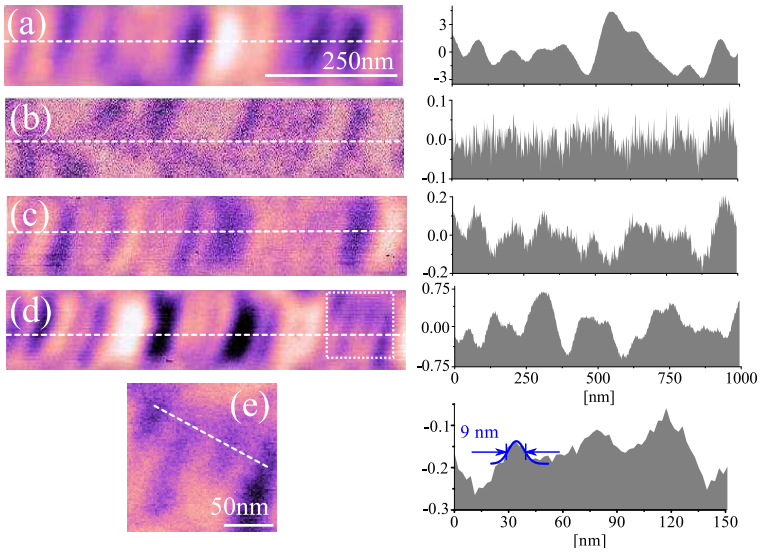

Figure 2. MFM images of a high density hard drive obtained with (a) commercial MFM probes, (b)–(d) t_n 5 nm, 10 nm and 15 nm thick Co-coated MFM-CNT tips, respectively. All scans were 1 μm in length. In each case, the cross-sectional profile corresponds to the line indicated on each image, showing the resolution as a function of the Co thickness. (e) Zoom on the area indicated in (d), showing the intersection of several bits, and sub-10 nm resolution for the t_n = 15 nm Co-coated MFM-CNT tip. The profile is 10 line average cross section.

Using these high resolution MFM-CNT tips, we then imaged micropatterned permalloy elements. As shown in figure 3(a, b), with commercial MFM tips it is difficult to determine the real structure of soft magnetic materials. The stray field of the tip is strong enough to perturb the magnetic state, displacing the domain walls and vortex core during imaging [21]. As a result of this interaction, the domain walls are observed as curved lines, bent towards the tip scanning direction. Furthermore the vortex core in the middle of the flux closure structure is not visible as the interaction with the tip distorts the image leading to poor resolution at the center of the structure. However, with a t_n = 15 nm Co-coated MFM-CNT tip, the details of the spin structures including the Néel walls, cross-tie walls and a vortex core can be observed with a very high level of detail, as can be seen in figure 3(c–d) . The domain walls appear as separated double lines, as expected from micromagnetic simulations [22] and theoretical calculations [21], and are completely straight, as previously shown by non-intrusive high resolution imaging [20, 23]. For the cross-tie structure in rectangular micropatterned permalloy elements, antivortex cores and their corresponding subdomain walls, 12–15 nm in width, are clearly resolved (figure 3(e,f)). We note that the location and shape of each particular spin nanostructure did not change even after repeated scans, confirming significant reduction of the stray fields produced by the MFM-CNT tips compared to commercial MFM tips, minimizing the impact of the scan on the spin structure while

retaining very good contrast. This improved imaging of complex spin structures in soft magnetic materials achieved with MFM-CNT tips, as mentioned by Kuramochi *et al.* [15], is not only a result of their high resolution and low perturbative effects because of their small magnetic volume, but also due to the high magnetic anisotropy of the tips, collinear with the magnetization of the imaged domain walls or vortex cores. Whereas commercial MFM tips require magnetic poling in an external field prior to imaging to achieve the highest quality scans (with $\sim$ 30 nm resolution), the t_n = 15 nm MFM-CNT tips show equivalent sub-10 nm resolution and high image quality with or without magnetization in an external field.

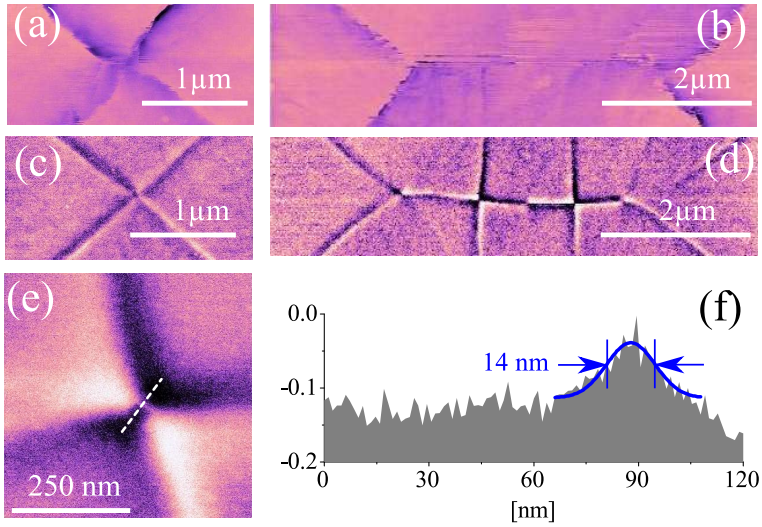

Figure 3. MFM images of the square and rectangular micropatterned elements in permalloy thin film obtained by ((a), (b)) a commercial MFM tip and ((c)–(e)) a 15 nm Co-coated CNT tip. (e), (f) Close up image of an antivortex core imaged with the 15 nm Co-coated CNT tip.

We emphasize that all these results, comparable or better than previous reports of maximum MFM resolution under ultra-high vacuum [16, 12, 14], were here obtained under ambient conditions, without vacuum or humidity control beyond those of a standard laboratory. The magnetic tips based on single-walled CNT with molecular beam epitaxy deposition of highly uniform Co layers thus have a clear advantage over the multi-walled tips demonstrated in previous studies [13, 16]. Although as a result of their small diameters, these tips are expected to outperform standard MFM tips or multi-walled MFM-CNT tips in all environments, their high imaging quality at ambient conditions is particularly promising for the implementation of MFM-CNT tips to characterize magnetic nanostructures without a cumbersome ultra-high vacuum environment. For instance, for the analysis of storage media quality at industrial scales, where rapid throughput requirements make the additional steps of pumping, transfer and positioning in a vacuum chamber undesirable, such tips could be particularly appealing.

4. Theoretical modelling

To interpret our experimental observations, and to understand the underlying mechanisms leading to the outstanding performance of the MFM-CNT tips, we modeled the tip-sample interaction, and the effect of the Co layer thickness on the resolution and contrast of the MFM image. In MFM dynamic mode, the magnetic interaction is detected by the phase shift of the cantilever oscillation, $\Delta\varphi$, which is proportional to gradient of the vertical force acting on the tip [24] $\Delta\varphi = -(Q/k) \cdot \partial F_z/\partial z$, where Q is the quality factor, k is the cantilever spring constant and the z-axis is chosen along the axis of the tip. The total magnetic force acting on the tip due to the interaction of its magnetization $\vec{m}(\vec{r})$ with that of the sample $\vec{m}'(\vec{r}')$ is:

$$F_z = \int_{\text{tip}} d^3r \int_{\text{sample}} d^3r'\, F_z^{ij}(\vec{r}-\vec{r}')m_i(\vec{r})m_j'(\vec{r}'), \tag{1}$$

where $\hat{F}_z(\vec{r}-\vec{r}') \sim 1/|\vec{r}-\vec{r}'|^4$ describes the vertical component of the dipole-dipole interaction [25].

Although in general the specific magnetic geometry of the tip should be considered, the highly elongated shape and small diameter of the thin Co-coated CNT tips permit a point-probe approximation [24, 26]. We investigate the MFM-CNT tip as a point dipole of radius $d_n/2$, and total magnetic moment $M = (1/6)\pi d_n^3 m_{\text{sat}}$ aligned along the tip axis [24, 26, 27]. Moreover, since in our experimental studies we consider only thin film samples, the 3D integral in Eq. (2) can be reduced to 2D, finally giving the phase shift in ideal (i.e., noiseless) MFM measurements as:

$$\Delta\varphi_0(\vec{r}) = -(1/6)\pi d_n^3 m_{\text{sat}} \frac{Q}{k}\frac{\partial}{\partial z}\int_{\text{sample}} d^2r'\, F_z^i(\vec{r}-\vec{r}')m_i'(\vec{r}')\Big|_{z=d_n/2+d}, \tag{2}$$

where d is the distance from the magnetic layer to the sample.

However, to obtain a realistic picture of the tip-sample interactions, we have to additionally take into account the inherent fluctuations of the measured system: thermal noise due to the vibration of the tip and cantilever, the roughness of the sample surface, as well as local variations of the magnetic properties, all neglected in previous studies [13, 16]. To quantify the noise level and clarify its origin we extracted its statistical distribution from the signal experimentally measured on uniformly in-plane-magnetized permalloy thin films with MFM-CNT tips, as shown in figure 4(a). First, we find that the probability distribution of the phase deviation of the cantilever oscillation $\delta\varphi \equiv \Delta\varphi - \langle\Delta\varphi\rangle$ is well described by a Gaussian distribution $\mathbb{P}(\delta\varphi) \propto \exp\left(-\delta\varphi^2/2\langle\delta\varphi^2\rangle\right)$ with the phase dispersion $\sqrt{\langle\delta\varphi^2\rangle} \simeq 0.05^\circ$ (figure 4(b)).

Moreover, we observe that the noise is highly local: the ensemble averaged correlation function of the phase deviations $G(\vec{r}) \equiv \langle\delta\varphi(0)\delta\varphi(\vec{r})\rangle$ has zero correlation length, as shown in figure 4(c). Meanwhile, we can independently estimate the minimum detectable force gradient for thermally limited measurements following Hug *et al.* [27] as: $\sqrt{\langle\delta\varphi^2\rangle} = \sqrt{Qk_BT\Delta\nu/k\omega_0A^2}$, where the tip oscillation amplitude $A = 10$ nm, its quality factor $Q = 350$, the measurement temperature $T = 300$ K, the bandwidth

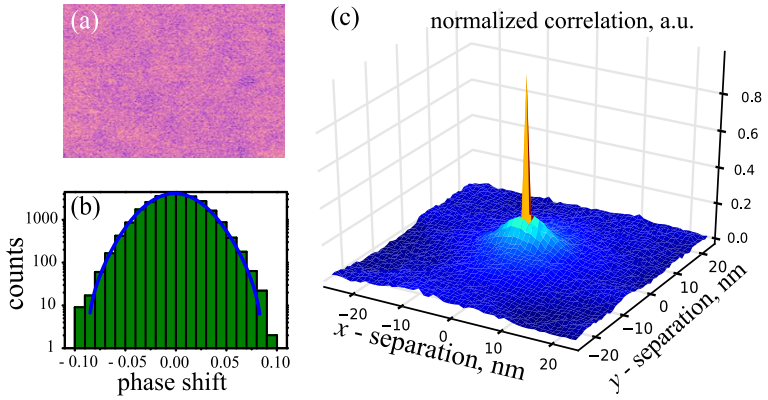

Figure 4. Statistical analysis of the noise of MFM-CNT measurements. (a) MFM image acquired on a uniformly in-plane-magnetized permalloy film. (b) The distribution of values of the phase deviation from its mean for the signal measured in (a), well fitted by a Gaussian function. (c) Spatial ensemble averaged correlation function of the phase noise. The strong peak at the zero coordinate separation suggests that the main contribution originates from thermal noise. The height of the correlation function peak is independent of the sample and magnetic layer thickness, likewise indicating that the main contribution comes from the thermal noise of the cantilever.

$\Delta\nu = 100$ Hz, the resonance frequency $\omega_0 = 75$ kHz, and the spring constant of the cantilever $k = 3.5$ N/m are all known parameters of the experimental measurement. We find that this estimate yields the same value as that determined experimentally on the permalloy samples. Thus, since the experimental noise is Gaussian, local, and appears to coincide perfectly with the theoretical estimate for the thermal noise, we conclude that its source is primarily the temperature fluctuations of the cantilever.

We can therefore complete our theoretical model by adding together the ideal phase shift [28] of the noiseless magnetic tip-sample interaction and the noise represented by a sampled Gaussian random phase shift with the value of the dispersion: $\Delta\varphi(\vec{r}) = \Delta\varphi_0(\vec{r}) + \delta\varphi(\vec{r})$ found above, where $\langle\delta\varphi(\vec{r})\delta\varphi(\vec{r}')\rangle = (Qk_BT\Delta\nu/k\omega_0A^2)\delta_{\vec{r}\vec{r}'}$. Using this model, we can now properly evaluate the resolution (the size of the minimal detectable magnetic feature) for a given CNT-based tip, allowing us to predict the capabilities and ultimate limits of MFM-CNT tips in real measurements.

To determine the resolution of a tip, we model the phase profile of a stripe of up- and down-oriented vertical magnetic domains in a thin film, as shown in figure 5(a, c), with different feature size D. Using the simulated profile, we define the resolution δ as the minimal feature size for which the contrast C, i.e. the difference between maximum and minimum phase shifts, is 50% larger than the noise level $\sqrt{\langle\delta\varphi^2\rangle}$ (or simply larger than zero for the noiseless situation), as shown in figure 5(b, d). We performed simulations for three situations: the ideal case neglecting noise effects, noise-limited measurement in air (quality factor $Q = 350$), and noise-limited measurement in vacuum (quality factor $Q = 3500$).

The significant role of the thermal noise of the cantilever in MFM imaging with CNT-based tips can be clearly seen from the dependence of the resolution on the Co layer

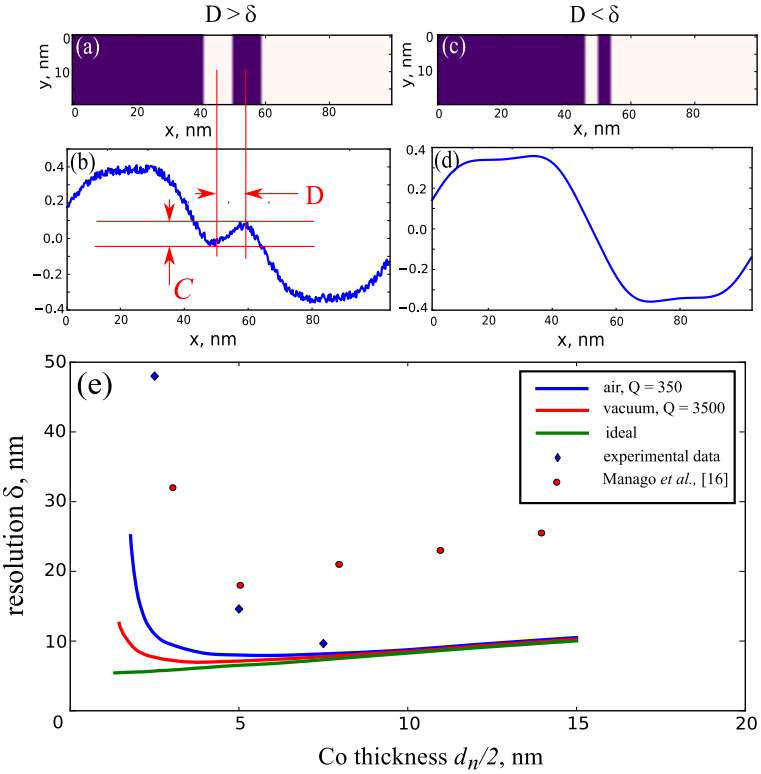

Figure 5. Determination of the resolution using the phase shift profile of a simulated magnetic domain structure. (a), (c) Simulated magnetic stripes in a thin film with magnetization perpendicular to the film plane, and varying feature size D. (b), (d) Corresponding phase cross-section and contrast C. Note that for small enough D, features will not be resolved even in the absence of noise. (e) Resolution vs. magnetic coating thickness from theoretical calculation and experimental data for single-walled and multi-walled MFM-CNT tips. Blue, red and green lines correspond to MFM measurements in the presence of thermal noise in air and vacuum, and ideal MFM measurements in vacuum at 4 K, respectively.

thickness, figure 5(e). For an ideal situation, the resolution of the image increases as the tip radius decreases, and thus the effective size of the tip dipole decreases, suggesting that the smallest possible tips should be fabricated for optimal imaging §. However, if we take into account noise during the image acquisition, maximum resolution is in fact obtained for a finite tip radius with intermediate magnetic coating thickness. This latter scenario is in excellent agreement with our experimental observations. As shown in figure 5(e), for both our single-walled MFM-CNT tips, and past work with larger-radius multi-walled CNT coated with a CoFe thin film, resolution decreases for both the largest and smallest tip radii, with optimal image quality obtained for ferromagnetic film coatings 6–18 nm thick.

Finally, to develop a clearer picture of the MFM-CNT tip-sample interaction and to compare it directly with our experimental results, we modeled the phase image of

§ The resolution does not become zero for the thinnest Co layers modeled, since we have a finite fixed distance from the tip to sample.

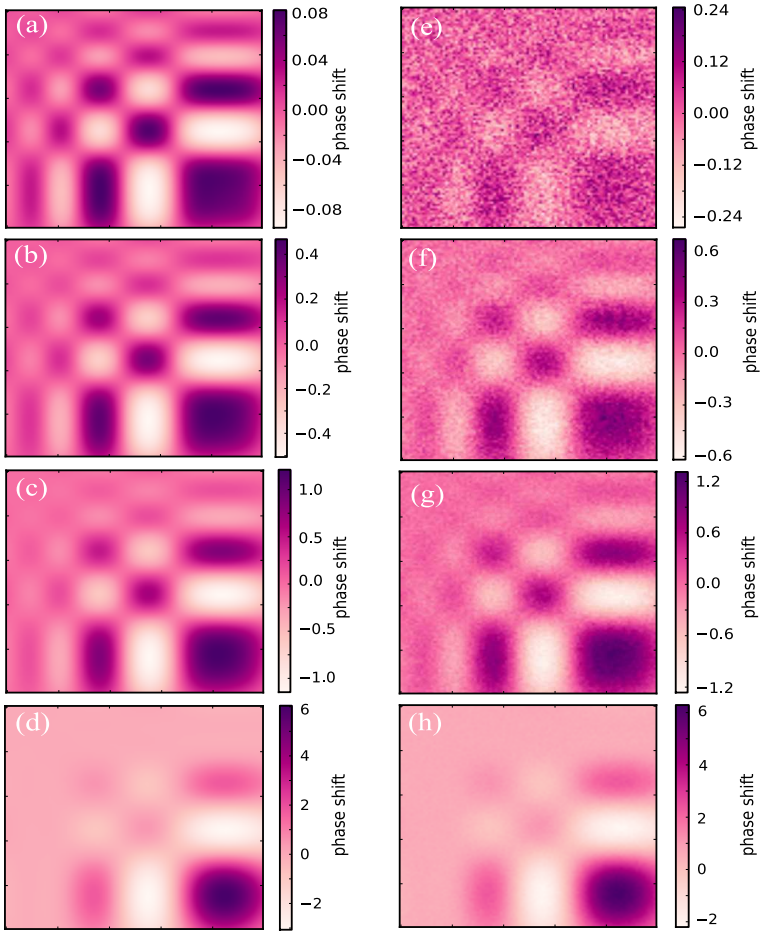

Figure 6. Simulated MFM image of perpendicularly oriented magnetic domains in thin film for MFM-CNT tips with $t_n = 5$, 10, 15 and 40 nm in the (e)–(h) presence and (a)–(d) absence of thermal noise, respectively. One clearly sees that in absence of the noise the best resolution is achieved for smallest tip (a), while in the presence of the thermal noise, the best resolution is achieved for a tip of finite thickness (g) of approx. $t_n \simeq 15$ nm in line with the experimental results. Each image is 100×100 nm^2.

a magnetic surface with up- and down-oriented vertical magnetic domains of variable 5–35 nm width, with finite 2 nm domain walls. The calculated MFM image with a 1 nm pixel size is illustrated in figure 6, as a function of the magnetic coating layer thickness. We note that, as in figure 5(e), the resolution of larger tips is practically independent of the strength of noise and simply proportional to the thickness of the magnetic coating, giving almost identical images for figure 6(d vs. h). In the ideal noiseless case, as the magnetic layer thickness decreases, resulting in smaller and smaller tip sizes, the image quality continues to improve, figure 6(c, b, a). However, as soon as measurement noise is included in the model, an optimal, finite magnetic layer coating gives the best quality images, figure 6(g vs. f,e), in agreement with the experimentally observed non-linear dependence of MFM resolution of the magnetic coating layer thickness.

5. Conclusions

In summary, using molecular beam epitaxy deposition of homogeneous and uniform magnetic coating layers on single-walled CNT, we have fabricated very sensitive and non-perturbative MFM-CNT tips with small magnetic volume and high magnetic anisotropy. Such tips allow for ultra-high sub-10 nm resolution imaging of magnetic nanostructures in soft and hard magnetic thin films. To understand the mechanism of image formation leading to this outstanding performance, we constructed a theoretical model of the tip-sample interaction, approximating the tip as a point-probe, and including hitherto neglected effects of thermal noise, which is shown to be the dominant factor limiting measurement sensitivity. This model, in excellent agreement with experimental observations, allows for a quantitative calculation of the magnetic coating layer thickness necessary for optimal imaging under a given set of measurement conditions. Based on our results, such specifically tailored tips can be controllably and reproducibly fabricated, and readily integrated into existing MFM platforms to produce the next generation of high-resolution magnetic probes.

Acknowledgments

The authors thank S. Cherifi and M. Longobardi for helpful discussions of spin structures in permalloy thin films.
This work was funded by the Swiss National Science Foundation (SNSF) through the NCCR MaNEP and Division II grants 200021-121750 and 200020-138198 and the EU (ERC-2007-StG 208162, MAGWIRE FP7-ICT-2009-5 257707; IFOX FP7-NMP3-LA-2010 246102).

References

[1] Bader S D. *Colloquium* : Opportunities in nanomagnetism. *Rev. Mod. Phys.*, 78:1–15, 2006.

[2] Novosad V, Grimsditch M, Darrouzet J, Pearson J, Bader S D, Metlushko V, Guslienko K, Otani Y, Shima H, and Fukamichi K. Shape effect on magnetization reversal in chains of interacting ferromagnetic elements. *Applied Physics Letters*, 82(21):3716–3718, 2003.

[3] Parkin S S P, Hayashi M, and Thomas L. Magnetic domain-wall racetrack memory. *Science*, 320(5873):190–194, 2008.

[4] Allwood D A, Xiong G, Faulkner C C, Atkinson D, Petit D, and Cowburn R P. Magnetic domain-wall logic. *Science*, 309(5741):1688–1692, 2005.

[5] http://www.seagate.com/files/docs/pdf/datasheet/disc/ds-cheetah-15k-5-us.pdf/.

[6] Gomez R D, Luu T V, Pak A O, Kirk K J, and Chapman J N. Domain configurations of nanostructured permalloy elements. *Journal of Applied Physics*, 85(8):6163–6165, 1999.

[7] Shinjo T, Okuno T, Hassdorf R, Shigeto K, and Ono T. Magnetic vortex core observation in circular dots of permalloy. *Science*, 289(5481):930–932, 2000.

[8] Cherifi S, Herte R, Kirschner J, Wang H, Belkhou R, Locatelli A, Heun S, Pavlovska A, and Bauer E. Virgin domain structures in mesoscopic co patterns: Comparison between simulation and experiment. *Journal of Applied Physics*, 98(4):043901, 2005.

[9] Lai M-F, Wei Z-H, Wu J C, Shieh W Z, Chang C R, and Guo J. Field evolution of multivortex and cross-tie states in permalloy thin films. *Journal of Applied Physics*, 101(9):09N111, 2007.

[10] Shigeto K, Okuno T, Mibu K, Shinjo T, and Ono T. Magnetic force microscopy observation of antivortex core with perpendicular magnetization in patterned thin film of permalloy. *Applied Physics Letters*, 80(22):4190–4192, 2002.

[11] Deng Z, Yenilmez E, Leu J, Hoffman J E, Straver E W J, Dai H, and Moler K A. Metal-coated carbon nanotube tips for magnetic force microscopy. *Applied Physics Letters*, 85(25):6263–6265, 2004.

[12] Kuramochi H, Uzumaki T, Yasutake M, Tanaka A, Akinaga H, and Yokoyama H. A magnetic force microscope using cofe-coated carbon nanotube probes. *Nanotechnology*, 16(1):24, 2005.

[13] Choi S J, Kim K H, Cho Y J, Lee H, Cho S, Kwon S J, Moon J, and Lee K J. Demonstration of ultra-high-resolution mfm images using co90fe10-coated cnt probes. *Journal of Magnetism and Magnetic Materials*, 322(3):332 – 336, 2010.

[14] Kuramochi H, Akinaga H, Semba Y, Kijima M, Uzumaki T, Yasutake M, Tanaka Ai, and Yokoyama H. Cofe-coated carbon nanotube probes for magnetic force microscope. *Japanese Journal of Applied Physics*, 44(4A):2077–2080, 2005.

[15] Kuramochi H, Manago T, Koltsov D, Takenaka M, Iitake M, and Akinaga H. Advantages of cnt–mfm probes in observation of domain walls of soft magnetic materials. *Surface Science*, 601(22):5289 – 5293, 2007.

[16] Manago T, Asada H, Uzumaki T, Takano F, Akinaga H, and Kuramochi H. The advantages of the magnetic structure in ferromagnetic-film-coated carbon nanotube probes. *Nanotechnology*, 23(3):035501, 2012.

[17] Hafner J H, Cheung C L, and Lieber C M. Direct growth of single-walled carbon nanotube scanning probe microscopy tips. *Journal of the American Chemical Society*, 121(41):9750–9751, 1999.

[18] Supplementary data.

[19] Wolny F, Mühl T, Weissker U, Lipert K, Schumann J, Leonhardt A, and Büchner B. Iron filled carbon nanotubes as novel monopole-like sensors for quantitative magnetic force microscopy. *Nanotechnology*, 21(43):435501, 2010.

[20] Kläui M and Vaz C A F. *Magnetization Configurations and Reversal in Small Magnetic Elements*. John Wiley & Sons, Ltd, 2007.

[21] Garcia J M, Thiaville A, Miltat J, Kirk K J, Chapman J N, and Alouges F. Quantitative interpretation of magnetic force microscopy images from soft patterned elements. *Applied Physics Letters*, 79(5):656–658, 2001.

[22] Donahue M J. Micromagnetic investigation of periodic cross-tie/vortex wall geometry. *Advances in Condensed Matter Physics*, (8):908692, 2012.

[23] Kronmüller H. *General Micromagnetic Theory*. John Wiley & Sons, Ltd, 2007.

[24] Hartmann U. The point dipole approximation in magnetic force microscopy. *Physics Letters A*, 137(9):475 – 478, 1989.

[25] Jackson J D. *Classical electrodynamics*. Wiley, 3 edition, 1998.

[26] Mamin H J, Rugar D, Stern J E, Terris B D, and Lambert S E. Force microscopy of magnetization patterns in longitudinal recording media. *Applied Physics Letters*, 53(16):1563–1565, 1988.

[27] Hug H J, Stiefel B, van Schendel P J A, Moser A, Hofer R, Martin S, Guntherodt H J, Porthun S, Abelmann L, Lodder J C, Bochi G, and O'Handley R C. Quantitative magnetic force microscopy on perpendicularly magnetized samples. *Journal of Applied Physics*, 83(11):5609–5620, 1998.

[28] Ovchinnikov D V and Bukharaev A A. Computer simulation of magnetic force microscopy imageswith a static model of magnetization distribution and dipoledipole interaction. *Technical Physics*, 46(8):85, 2001.